Received: 22 September 2025 | Revised: 15 November 2025 | Accepted: 28 November 2025

https://doi.org/10.56946/jce.v4i2.827

Journal of Chemistry and Environment

Research Article

Green-Synthesized Iron Oxide Nanoparticles from Olive Leaves for Efficient Photocatalytic Degradation of Dyes and Chlorpyrifos

Aiman Niaz*[1], Muhammad Suleman*[1], Rahim Ullah[2]

[1]Department of Agricultural Chemistry and Biochemistry, The University of Agriculture Peshawar KPK Pakistan, 25000.
[2]Department of Chemistry and Molecular Sciences, 00560, University of Helsinki, Finland.

*Correspondence: (Aiman Niaz)
aiman@aup.edu.pk

Abstract

This study investigated the green synthesis of iron oxide nanoparticles using olive leaf extract and their application in degradation of synthetic dyes and chlorpyrifos. The nanoparticles were characterized by UV–visible spectrophotometry, FTIR, XRD, and SEM. UV–visible analysis revealed a distinct absorption peak near 300 nm, while FTIR confirmed functional groups including hydroxyl, carbonyl, nitrile, and alkyne. XRD showed well-defined diffraction peaks at planes (131), (113/247), (125), (393/138), (622), and (118), indicating a crystalline structure. SEM images revealed uniformly dispersed spherical nanoparticles with sizes ranging from 20 to 100 nm. Under light conditions, the nanoparticles exhibited significant degradation of methyl orange, methyl red, Congo red, and chlorpyrifos, with the highest degradation observed for methyl red (34.28%) and chlorpyrifos (27.38%) after 120 minutes. Our results demonstrate the potential of olive leaf–mediated iron oxide nanoparticles for pollutant degradation, while further studies on mineralization, reusability, and by-product analysis are needed to fully evaluate their environmental applicability.

Keywords: Green synthesis, olive leaves, iron oxide nanoparticles, photodegradation.

1. Introduction

Rapid industrial expansion, urbanization, and population growth have intensified the release of harmful pollutants into the environment [1, 2]. Synthetic dyes are among the most persistent contaminants due to their complex molecular structures, which include chromophore and auxochrome groups [3]. Based on their chemical composition, dyes are commonly categorized into azo, anthraquinone, indigo, and other classes. Although natural dyes were used for millennia, the last 150 years have seen a shift toward synthetic dyes for textile and tannery applications [4]. Today, the textile industry alone produces about 7×10^7 tons of dyes annually, and nearly 10% of this quantity is discharged into water systems during processing [5]. Even at low concentrations dye-contaminated wastewater poses serious ecological risks. It reduces light penetration, disrupts photosynthesis, increases biochemical and chemical oxygen demand, and affects plant and aquatic life. Many artificial dyes are highly stable, bioaccumulative, and exhibit toxic, mutagenic, or carcinogenic effects [6]. Pesticides create similar environmental concerns. Their widespread use in modern agriculture contributes to soil degradation, loss of biodiversity, and contamination of food and water. Chlorpyrifos, a widely used organophosphate pesticide, is especially problematic due to its toxicity and persistence [7]. Repeated exposure alters soil microbial communities and threatens non-target species. It is one of the most frequently detected pesticide residues in environmental and agricultural samples, prompting increasing concern and the need for safer remediation approaches [8].

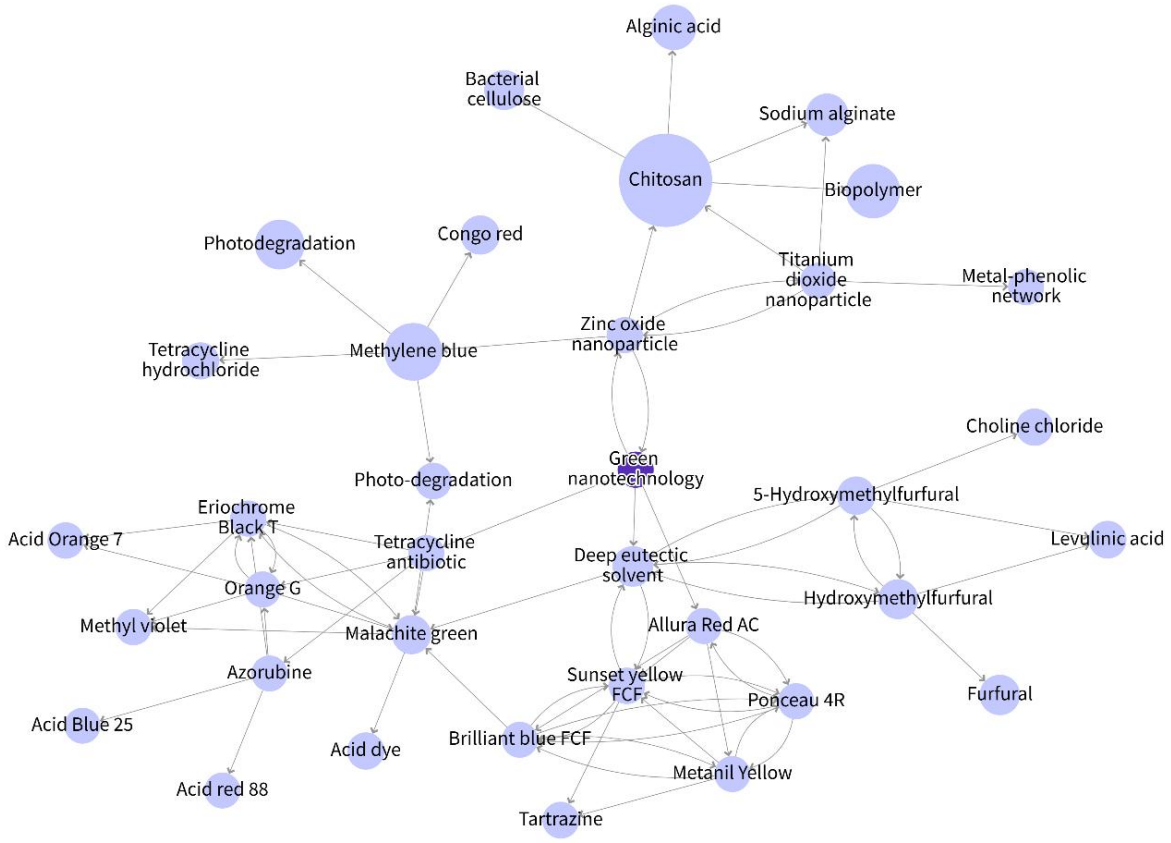

Figure 1. Research landscape from early 2000s to the present of green nanoparticles in environmental pollutant degradation (source web of science)**.**

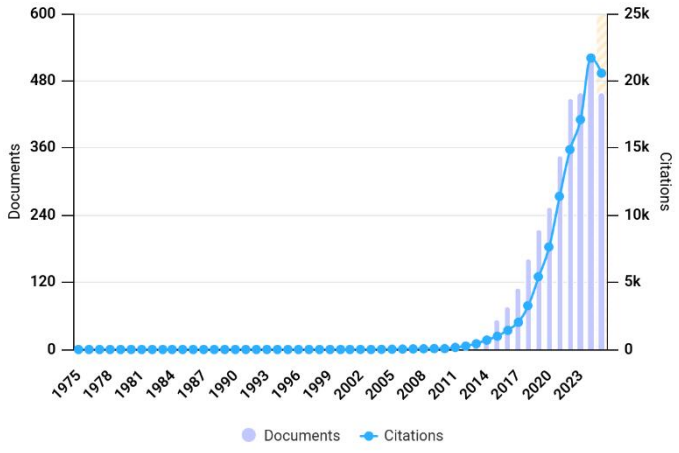

Figure 2. Annual publication trends from early 2000s to the present: green nanoparticle-Based pollutant degradation research (source web of science)

Nanoparticles have emerged as promising tools for environmental cleanup because of their small size, large reactive surface area, and tunable physicochemical properties [9, 10]. As their applications expand, there is growing interest in synthesis routes that avoid toxic chemicals and reduce environmental impacts [11]. Green synthesis as an emerging method (figure 1), which uses plant extracts or other biological agents, offers a sustainable alternative to conventional physical and chemical nanoparticle production methods [12, 13]. Previous studies highlight the potential of green-synthesized nanoparticles for pollutant degradation and environmental applications Figure 2 and 3 [14]. Olive leaves contain a high level of phenolic and flavonoid compounds, that act as strong reducing and stabilizing agents [15]. They are also an inexpensive agricultural by-product, making them a sustainable choice. Therefore, present study aimed to synthesize iron oxide nanoparticles using olive leaf extract and assess their effectiveness in degrading three synthetic dyes: methyl orange, methyl red, and Congo red and the pesticide chlorpyrifos. This work contributes to developing environmentally friendly remediation strategies based on green nanotechnology.

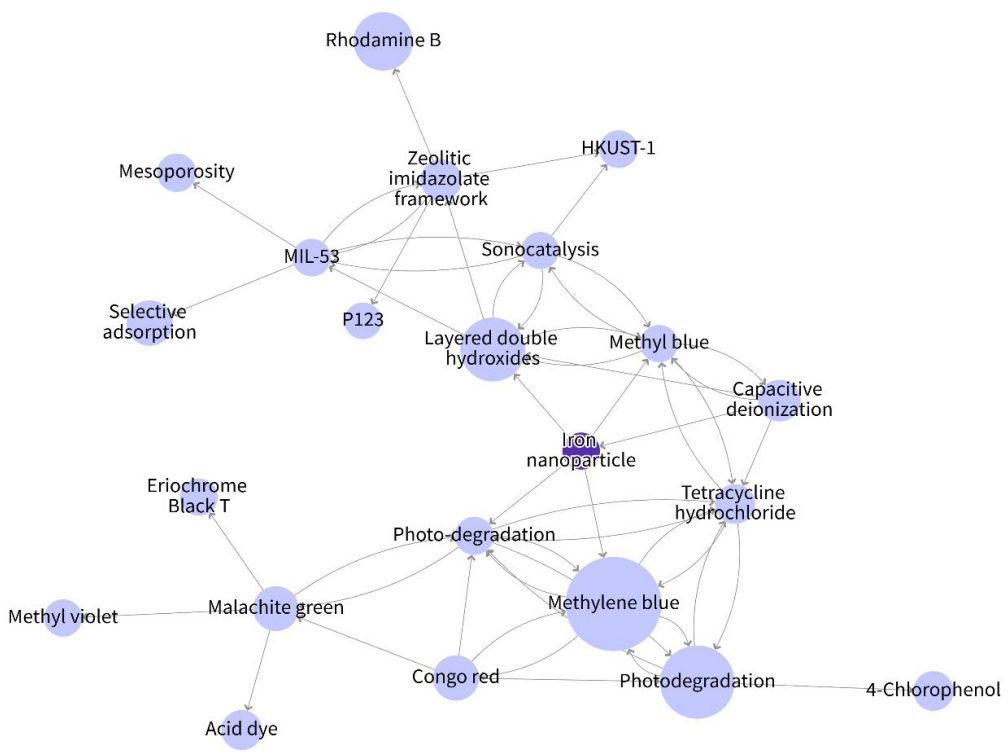

Figure 3. Research landscape from early 2000s to the present of green iron Oxide nanoparticles in environmental pollutant degradation (source web of science).

2. Materials and methods

2.1. Collection and Preparation of Olive Leaf Extract

Olive leaves were collected from the Agricultural University Peshawar, Malakander Farm. The leaves were washed with distilled water, air-dried in the shade, and then ground into a fine powder. To prepare the extract, 15 g of leaf powder were mixed with 250 mL of distilled water in a beaker and stirred using a magnetic stirrer. The mixture was heated for one hour and then filtered to obtain the aqueous olive leaf extract. This extract was used for subsequent nanoparticle synthesis.

2.2. Green Synthesis of Iron Oxide Nanoparticles

Iron oxide nanoparticles were synthesized by reacting an iron salt solution with the olive leaf extract, which served as both the reducing and stabilizing agent. A 0.1 M solution of ferrous sulfate was prepared by dissolving 13.9 g of $FeSO_4$-$7H_2O$ in 500 mL of distilled water. The olive leaf extract was then mixed with this solution in a reaction vessel. The mixture was subjected to controlled heating using microwave irradiation for a set duration During heating, the phytochemicals in the extract facilitated the reduction and stabilization of iron ions, leading to nanoparticle formation. Successful synthesis was indicated by a visible color change from pale yellow to dark brown or black. The nanoparticles were then stored for subsequent characterization and applications.

2.3 UV-vis spectroscopy analysis

Initial characterization of the iron oxide nanoparticles was confirmed using UV-VIS spectroscopy within the 200-800 nm wavelength range [16]. A diluted suspension of the nanoparticles was prepared in an appropriate solvent, and the spectrophotometer settings were adjusted accordingly. The sample was transferred into a quartz cuvette and scanned across the selected wavelength range. The resulting absorbance spectrum showed characteristic peaks associated with iron oxide nanoparticles, which were compared with reference spectra and published reports for confirmation.

2.4 Scanning Electron Microscopy (SEM) Analysis

The morphology and surface features of the synthesized iron oxide nanoparticles were examined using Scanning Electron Microscopy [17]. A diluted nanoparticle suspension was placed

on a clean substrate and air-dried to form a uniform film. The dried sample was mounted on an SEM stub using conductive adhesive and coated with a thin conductive layer of gold or carbon. The specimen was then placed in the SEM chamber, and imaging parameters were adjusted before capturing high-resolution micrographs. Imaris software was used to measure particle size, morphology, and aggregation patterns.

2.5 Xray Diffraction (XRD) analysis

The structural characteristics of the synthesized iron oxide nanoparticle were examined through Xray Diffraction (XRD) analysis[18]. The dried nanoparticle powder was finely ground and sieved to achieve uniform particle size before being placed into the sample holder. The instrument was set up using Cu Kα radiation (λ = 1.5406 Å) with appropriate voltage and current settings. Diffraction data were collected over a 2θ range of 10° to 80°. The resulting patterns were analyzed to identify crystal phases and determine structural features. Diffraction peaks were indexed using standard crystallographic databases, allowing calculation of lattice parameters and assessment of crystallinity. Information on composition, purity, crystallite size, and overall structure was obtained through peak analysis and comparison with reference data.

2.6 Fourier Transform Infrared (FTIR) Spectroscopy

FTIR spectroscopy was used to determine the functional groups of the synthesized iron oxide nanoparticles [19]. The dried nanoparticle powder was mixed with potassium bromide (KBr), an infrared-transparent medium, to form a solid pellet for analysis. The instrument was calibrated and set to scan from 400 to 4000 cm^{-1} with a resolution of 4 cm^{-1}. The pellet was then placed in the sample holder, and spectra were recorded across the selected wavenumber range. The resulting infrared profile was examined to identify characteristic absorption bands associated with chemical bonds and molecular vibrations. These features were compared with reference spectra and published data to confirm the functional groups present in the iron oxide nanoparticles.

2.7 Degradation of dyes and chlorpyrifos

The degradation of synthetic dyes (methyl orange, methyl red, and Congo red) and the pesticide chlorpyrifos was evaluated using iron oxide nanoparticles synthesized from olive leaves. Stock solutions of 500 ppm for each dye and chlorpyrifos were prepared in distilled water and serially diluted to concentrations of 100, 50, and 25 ppm. For each assay, a measured volume of the prepared solution was mixed with a specified amount of the synthesized nanoparticles. The mixtures were homogenized and allowed to react for 0, 60, 90, and 120 minutes. The light source used for photocatalysis was a W-lamp operated above the samples. Degradation was monitored by UV–visible spectroscopy, recording absorbance spectra at each time interval. All experiments were performed in triplicate. Control assays included: dye/pesticide solutions without nanoparticles, (ii) nanoparticle suspensions kept in the dark, and (iii) blank measurements to account for background absorbance. These controls helped distinguish photocatalytic activity from natural photolysis. The percentage degradation was calculated using the formula described in previous studies [20, 21]. The following formula was used for calculation of percentage degradation:

$$\text{Degradation (\%)} = ((A - A_t) / A_0) \times 100$$

A_0 is the initial absorbance of the dye/ Chlorpyrifos.

A_t is the absorbance at a specific time point.

3. Results and discussion

3.1. Preparation of iron oxide NPs

The green synthesis of iron oxide nanoparticles (FeOx NPs) using olive leaf extract was highly efficient, thanks to the abundance of bioactive phytochemicals such as flavonoids, polyphenols, tannins, and glycosides in olive leaves [22]. These molecules perform a dual role; they reduce iron ions and simultaneously stabilize the growing nanoparticles which is consistent with their reported function in other plant-mediated syntheses [23, 24]. Phytochemicals such as flavonoids, polyphenols, tannins, and glycosides have been reported previously in olive leaves extracts [25, 26].Because of its interaction with metal ions, the phytochemicals facilitate the preparation of iron oxide nanoparticles which further leads to the preparation of black-colored precipitates [27] . we observed that during preparation the reduction of Fe^{3+} to Fe^0 does not occur directly when the iron salt was mixed with the leaf extract under specific reaction conditions. However, at P^H 7 the

highest amount of iron oxide nanoparticles synthesis was achieved. The UV spectrum of the iron oxide nanoparticles recorded for absorption peaks in the ultraviolet region, with a wavelength ranged between 200-400 nm which was 300 nm as mentioned in Figure 4. Previously in this range (200-400 nm) for iron oxide nanoparticle have been reported [28, 29]. This absorbance measurements within this range allowed for the assessment of the optical behavior and absorption characteristics of the nanoparticles [30]. In evidence of these previous studies, this also confirmed our successfully synthesis of iron oxide nanoparticles. Similarly, the obtained UV-spectrophotometer data, including the absorbance peaks and corresponding wavelengths, provided valuable information regarding the optical properties and bandgap of the synthesized iron oxide nanoparticles [31], thereby enhancing the overall understanding of their optical behavior.

3.2 FTIR analysis of Iron oxide nanoparticles

Iron oxide nanoparticles synthesized using extract of olive leaves were analyzed by Fourier-transform infrared spectroscopy (FTIR) to identify the functional groups present (Table 1 and Figure 5). The analysis of FTIR revealed the appearance of specific functional groups, with each group showed distinct characteristic wavelengths. The first functional group detected was alcohol (hydroxyl) with a wavelength of 1059 cm^{-1}. Hydroxyl groups (OH) known for their high reactivity in various chemical reactions [32], and facilitate oxidation as well as hydrolysis reactions [33].it acts as active sites for electron transfer which helps in breakdown of organic pollutants, including dyes and pesticides [34]. Similarly, carbonyl functional group was observed at a wavelength of 1607 cm^{-1}. Carbonyl groups (C=O) are highly reactive and can undergo oxidation-reduction reactions [35]. carbonyl groups can generate reactive oxygen species and play a vital role in electron transfer processes which contributes in degradation of dyes and pesticides by breaking down chemical bonds within the organic molecules [36]. Similarly, the presence of nitrile functional groups was detected at a wavelength of 1999 cm^{-1}. Nitrile functional groups can participate in hydrolysis or oxidative degradation reactions, contributing to the breakdown of dyes and pesticides [37].

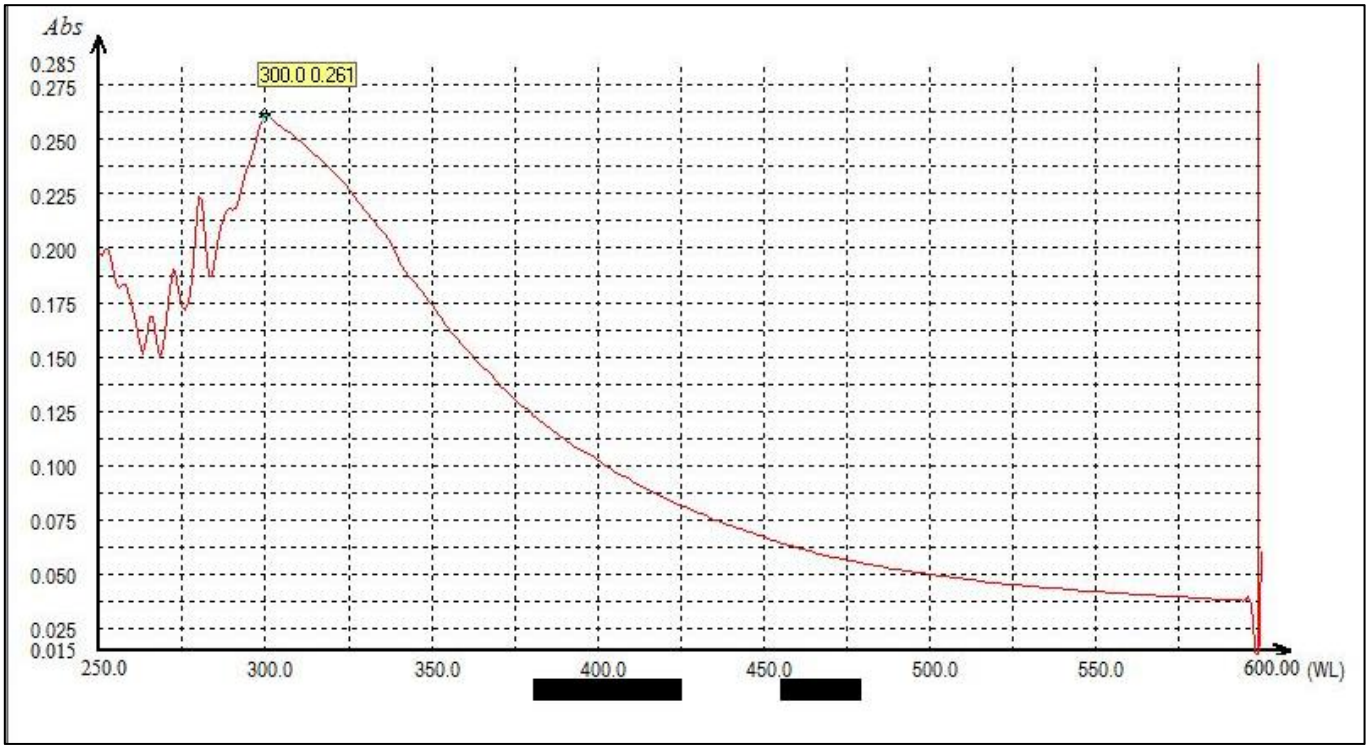

Figure 4. UV-spectra of iron oxide nanoparticles through spectrophotometer.

Table 1. Detected functional group in FTIR analysis of iron oxide nanoparticles.

S.No	Wavelength (cm^{-1})	Bond	Functional Group
1	1059	C-OH	Alcohol (Hydroxyl)
2	1607	C=O	Carbonyl
3	1999	C≡N	Nitrile
4	2201	C≡C	Alkyne
5	3235	O-H	Hydroxyl

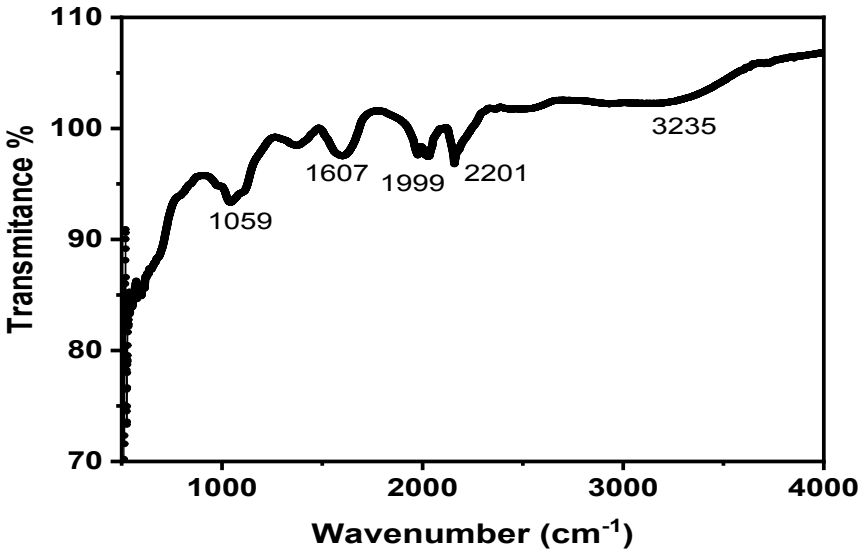

Figure 5. FTIR Spectra of iron oxide nanoparticles.

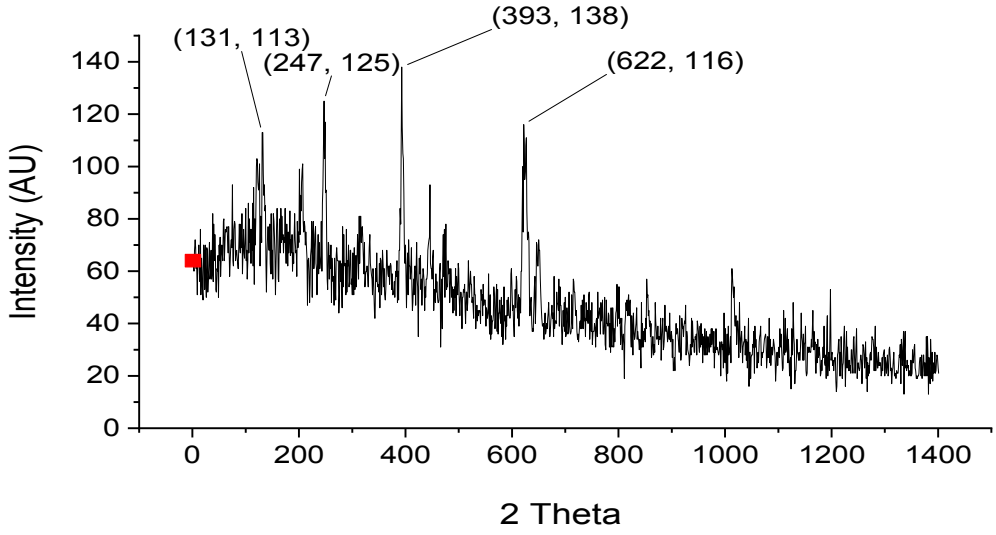

Figure 6. XRD analysis of green iron oxide nanoparticles.

The alkyne functional group was identified at a wavelength of 2201 cm^{-1}. Alkyne groups can aid in the cleavage of organic compounds, facilitating their breakdown into smaller, less harmful molecules [38]. Furthermore, the hydroxyl functional groups were detected at a wavelength of 3235 cm^{-1}. The presence of these specific functional groups in iron oxide nanoparticles shows its potential in the degradation of dyes and pesticides.

3.4 X-ray diffraction (XRD) of iron oxide nanoparticles

The X-ray diffraction (XRD) data is presented in Figure 6, which plays a significant part in unraveling the intricate synthesized nanoparticles crystal structure. The recorded XRD pattern reveals a series of distinct peaks at specific angles, namely 25.16°, 35.12°, 36.63°, 40.64°, 49.97°, 57.08°, and 59.42°.

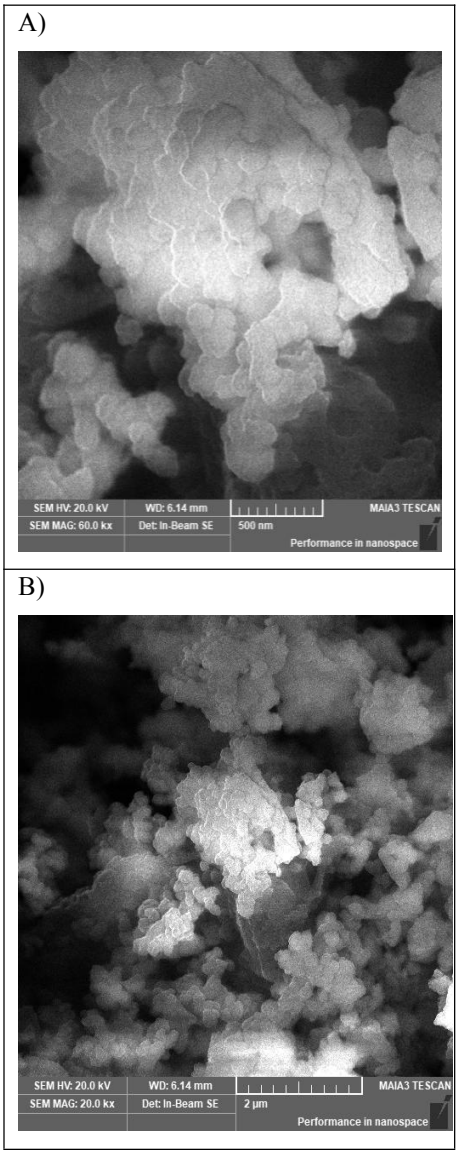

Figure 7. Scene electron microscopy of iron oxide nanoparticles (A) 500nm and (B) 2µm.

These peaks hold significant importance as they correspond to specific crystal planes, shedding light on the internal arrangement of atoms within the nanoparticles. The first peak at 25.16° corresponds to the (131) crystal plane, providing valuable information about the orientation and spacing of atoms along this specific direction. Similarly, the peak at 35.12° corresponds to the crystal planes (113, 247), indicating the presence of multiple planes and their relative orientation within the nanoparticle structure.

Furthermore, the peak observed at 36.63° corresponds to the (125) crystal plane, signifying the arrangement of atoms in yet another direction. Similarly, noteworthy are the peaks at 40.64°, which corresponds to the crystal planes (393, 138), and at 49.97°, which corresponds to the (622) crystal plane. These peaks contribute to a more understanding of the crystal lattice and the atomic arrangement in the synthesized nanoparticles.

Additionally, the peaks at 57.08° and 59.42° correspond to the (118) crystal plane, further enriching our knowledge of the crystal structure. Previously, same structural properties were reported in various studies [39-41]. Moreover, the FeO NPs was observed for peaks corresponding to crystal planes (113) and (247) in their XRD analysis [42], which is also present in this study results in this correspondence further supports the validity of this study findings and strengthens the understanding of iron oxide nanoparticle crystal structures. These findings strongly support the formation of iron oxide nanoparticles with well-defined peaks in the XRD pattern confirms the crystalline nature.

3.4 Scene electron microscopy (SEM) of iron oxide nanoparticles

The Scene Electron microscopy (SEM) of the iron oxide nanoparticles provided important insights into their morphology, size distribution, and surface characteristics [43]. A representative SEM image in Figure 7 A and B shows well-dispersed spherical particles with varying sizes, ranging from 20 to 100 nanometers. This indicated that the synthesis method employed was effective in achieving a uniform particle distribution. Further analysis of the SEM images allowed for the determination of important parameters such as particle size and size distribution [44]. The size distribution of the iron oxide nanoparticles shows a relatively narrow distribution with most particles centered around 50 nanometers. This size distribution was consistent with the observations from the SEM image, indicating a controlled synthesis process. These surface features significantly impact the reactivity and interaction of

the nanoparticles with other materials, making them essential considerations for various. The synthesized nanoparticles exhibited a uniform size distribution and distinct surface features, making them promising candidates for numerous uses in biomedicine, catalysis, and environmental amend. The SEM characterization results of the current study regarding the morphology, size distribution, and surface characteristics of iron oxide nanoparticles align with previous research in the field. These results are well support by Previous studies the synthesized nanoparticles were confirmed the size distribution of iron oxide nanoparticles [45, 46].

3.5 Degradation study of dyes and chlorpyrifos

The degradation efficiency of iron oxide nanoparticles (FeOx NPs) against synthetic dyes and the pesticide chlorpyrifos was systematically evaluated at different reaction intervals to assess their catalytic potential (Table 2 and figure 8). Among the dyes tested, Methyl Red exhibited the highest total degradation of 34.28% after 120 minutes. This enhanced degradation can be attributed to the chemical structure of Methyl Red, which contains functional groups more susceptible to attack by the catalytic surface of iron oxide nanoparticles [47]. Moreover, bioactive phytochemicals in the olive leaf extract likely enhanced the degradation process by promoting electron transfer and increasing reactive surface interactions, thereby accelerating the breakdown of dyes. [48]. Furthermore, the degradation efficiency of Methyl Red was influenced by its initial concentration and the duration of contact with the nanoparticles, with longer exposure promoting more extensive breakdown.

Similarly, Chlorpyrifos, a commonly used organophosphate pesticide, underwent significant degradation, with 27.38% reduction after 120 minutes. Pesticides generally possess more complex molecular structures, making their breakdown challenging [49]. However, plant-derived nanoparticles are decorated with multiple active phytochemical moieties that enhance surface reactivity and catalytic activity, enabling effective cleavage of chlorpyrifos bonds. In contrast, Methyl Orange and Congo Red showed slightly lower degradation efficiencies of 25.33% and 25.06%, respectively, after 120 minutes. These differences suggest that molecular structure and bond stability strongly influence susceptibility to nanoparticle-mediated degradation. Notably, the photocatalytic potential of iron oxide nanoparticles was evident, as degradation efficiency tends to improve under light exposure [50]. Previous studies have demonstrated similar photocatalytic applications of plant-extract-synthesized iron oxide nanoparticles for dye and pollutant degradation [51-53].

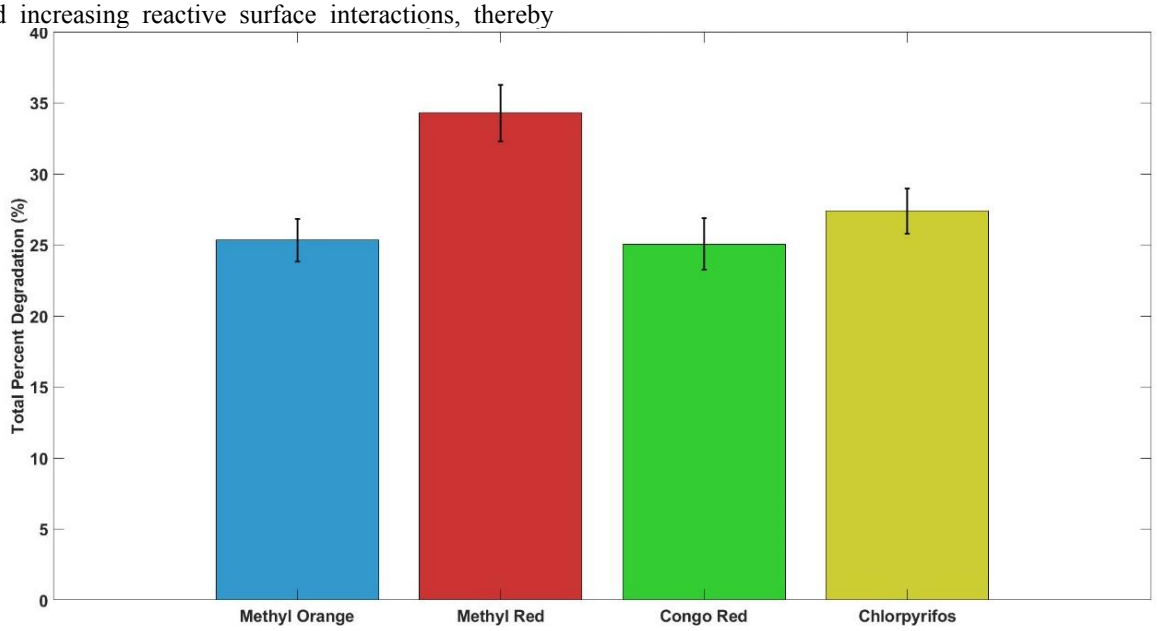

Figure 8. Total percent degradation of dyes and Chlorpyrifos.

Table 2. Time-dependent photocatalytic degradation of chlorpyrifos, Congo Red, Methyl Red, and Methyl Orange under controlled light conditions.

Sample	Reading Cycle	Absorbance	Degradation (%)	Total % degradation
Chlorpyrifos	Control	1.816	-	-
	Dark (30 min)	1.731	4.81	4.81
	30 min (light)	1.701	1.14	5.95
	60 min(light)	1.515	3.96	9.91
	90 min (light)	1.387	6.42	16.33
	120 min (light)	1.279	11.05	27.38
Congo red	Dark (30 min)	1.728	4.17	4.17
	30 min (light)	1.706	0.92	5.09
	60 min (light)	1.522	3.63	8.72
	90 min (light)	1.396	5.61	14.33
	120 min (light)	1.289	10.73	25.06
Methyl red	Dark (30 min)	1.721	5.22	5.22
	30 min (light)	1.693	1.63	6.85
	60 min (light)	1.512	10.71	17.56
	90 min (light)	1.379	8.80	26.36
	120 min (light)	1.271	7.92	34.28
Methyl orange	Dark (30 min)	1.731	4.81	4.81
	30 min (light)	1.708	0.46	0.46
	60 min (light)	1.538	1.55	7.25
	90 min (light)	1.411	7.23	13.51
	120 min (light)	1.309	12.31	25.33

.

However, the use of olive leaf extract as the synthesis source is novel, adding its phytochemicals that may contribute to enhanced catalytic activity. The observed variations in degradation among different pollutants highlight the importance of considering specific chemical structures and properties when designing nanoparticle-based remediation strategies [54]. Several plant extracts have been used to synthesize iron oxide nanoparticles, reported degradation efficiencies [55, 56]. Our findings demonstrate that green-synthesized iron oxide nanoparticles are promising candidates for sustainable environmental remediation, capable of effectively reducing the concentration of both dyes and pesticides in aqueous systems.

5. Conclusion

Our synthesized iron oxide nanoparticles showed potent degradation of dyes and chlorpyrifos under light conditions. While the results demonstrate promising catalytic activity, the study is limited by the absence of mineralization data, reusability testing, and a detailed analysis of degradation by-products. These aspects should be investigated in future work to fully establish their environmental applicability.

Authors Contribution

Aiman Niaz: Methodology-Formal Analysis-Writing – original draft. Muhammad Suleman: Project Supervision-Writing – review & editing, Validation. Rahim Ullah: Review & editing, visualization. All authors read and agreed on the published version of manuscript.

Conflicts of Interest

There are no conflicts of interest reported by the writers.

Funding: No funding support is available for this study.

Acknowledgment

We are thankful to The Agricultural Research Institute Tarnab, Peshawar Pakistan for providing us the facility in degradation part of this research.

Data Availability statement

The data present in this study are available on the request from corresponding author.

Ethical Approval

No Applicable

REFERENCES

1. Weldeslassie, T., et al., Chemical Contaminants for Soil, Air and Aquatic Ecosystem, in Modern Age

Environmental Problems and their Remediation, M. Oves, M. Zain Khan, and I. M.I. Ismail, Editors. 2018, Springer International Publishing: Cham. p. 1-22.
2. Naidu, R., et al., Chemical pollution: A growing peril and potential catastrophic risk to humanity. Environment International, 2021. 156: p. 106616.
3. Aslam, M., et al., How the dyes are degraded/mineralized in a photocatalytic system? The possible role of auxochromes. Water, Air, & Soil Pollution, 2015. 226: p. 1-15.
4. Clark, M., Handbook of textile and industrial dyeing: principles, processes and types of dyes. 2011: Elsevier.
5. Hashemi, S.H. and M. Kaykhaii, Chapter 15 - Azo dyes: Sources, occurrence, toxicity, sampling, analysis, and their removal methods, in Emerging Freshwater Pollutants, T. Dalu and N.T. Tavengwa, Editors. 2022, Elsevier. p. 267-287.
6. Ardila-Leal, L.D., et al. A Brief History of Colour, the Environmental Impact of Synthetic Dyes and Removal by Using Laccases. Molecules, 2021. 26, DOI: 10.3390/molecules26133813.
7. Ubaid ur Rahman, H., et al., A comprehensive review on chlorpyrifos toxicity with special reference to endocrine disruption: Evidence of mechanisms, exposures and mitigation strategies. Science of The Total Environment, 2021. 755: p. 142649.
8. John, E.M. and J.M. Shaike, Chlorpyrifos: pollution and remediation. Environmental Chemistry Letters, 2015. 13(3): p. 269-291.
9. Khin, M.M., et al., A review on nanomaterials for environmental remediation. Energy & Environmental Science, 2012. 5(8): p. 8075-8109.
10. Rafeeq, H., et al., Functionalized nanoparticles and their environmental remediation potential: a review. Journal of Nanostructure in Chemistry, 2022. 12(6): p. 1007-1031.
11. Chandrakala, V., V. Aruna, and G. Angajala, Review on metal nanoparticles as nanocarriers: current challenges and perspectives in drug delivery systems. Emergent Materials, 2022. 5(6): p. 1593-1615.
12. Hussain, I., et al., Green synthesis of nanoparticles and its potential application. Biotechnology Letters, 2016. 38(4): p. 545-560.
13. Peralta-Videa, J.R., et al., Plant-based green synthesis of metallic nanoparticles: scientific curiosity or a realistic alternative to chemical synthesis? Nanotechnology for Environmental Engineering, 2016. 1(1): p. 4.
14. Singh, P., et al., Systematic review on applicability of magnetic iron oxides–integrated photocatalysts for degradation of organic pollutants in water. Materials Today Chemistry, 2019. 14: p. 100186.
15. Markhali, F.S., J.A. Teixeira, and C.M.R. Rocha, Olive Tree Leaves—A Source of Valuable Active Compounds. Processes, 2020. 8(9): p. 1177.
16. Kebede, A., et al., Controlled synthesis, characterization, and application of iron oxide nanoparticles for oral delivery of insulin. Lasers in Medical Science, 2013. 28(2): p. 579-587.
17. Mahdavi, M., et al. Synthesis, Surface Modification and Characterisation of Biocompatible Magnetic Iron Oxide Nanoparticles for Biomedical Applications. Molecules, 2013. 18, 7533-7548 DOI: 10.3390/molecules18077533.
18. Saqib, S., et al., Synthesis, characterization and use of iron oxide nano particles for antibacterial activity. Microscopy Research and Technique, 2019. 82(4): p. 415-420.
19. Rajendran, S.P. and K. Sengodan, Synthesis and Characterization of Zinc Oxide and Iron Oxide Nanoparticles Using Sesbania grandiflora Leaf Extract as Reducing Agent. Journal of Nanoscience, 2017. 2017(1): p. 8348507.
20. Vigneshwaran, S., J. Preethi, and S. Meenakshi, Removal of chlorpyrifos, an insecticide using metal free heterogeneous graphitic carbon nitride (g-C3N4) incorporated chitosan as catalyst: Photocatalytic and adsorption studies. International Journal of Biological Macromolecules, 2019. 132: p. 289-299.
21. Neppolian, B., et al., Solar/UV-induced photocatalytic degradation of three commercial textile dyes. Journal of Hazardous Materials, 2002. 89(2): p. 303-317.
22. Al-Hamdani, H. and S.H. Ahmed, The effect of exposing dried olive (Olea europaea) leaves extract to

microwaves in the synthesis of iron oxide nanoparticles and its effect on the biological activity of different extracts of pathogenic bacteria. Biochemical & Cellular Archives, 2020. 20(1).

23. Yousaf, Z. and N. Saleh, Advanced Concept of Green Synthesis of Metallic Nanoparticles by Reducing Phytochemicals, in Nanobotany, S. Javad and A. Butt, Editors. 2018, Springer International Publishing: Cham. p. 17-36.
24. Koduru, J.R., et al., Phytochemical-assisted synthetic approaches for silver nanoparticles antimicrobial applications: A review. Advances in Colloid and Interface Science, 2018. 256: p. 326-339.
25. Rahmanian, N., S.M. Jafari, and T.A. Wani, Bioactive profile, dehydration, extraction and application of the bioactive components of olive leaves. Trends in Food Science & Technology, 2015. 42(2): p. 150-172.
26. Borjan, D., et al. Microbiological and Antioxidant Activity of Phenolic Compounds in Olive Leaf Extract. Molecules, 2020. 25, DOI: 10.3390/molecules25245946.
27. Sharma, R., et al., Potential applications of green-synthesized iron oxide NPs for environmental remediation. Environmental Monitoring and Assessment, 2023. 195(11): p. 1397.
28. Ismail, R.A., et al., Antibacterial activity of magnetic iron oxide nanoparticles synthesized by laser ablation in liquid. Materials Science and Engineering: C, 2015. 53: p. 286-297.
29. Amendola, V., P. Riello, and M. Meneghetti, Magnetic Nanoparticles of Iron Carbide, Iron Oxide, Iron@Iron Oxide, and Metal Iron Synthesized by Laser Ablation in Organic Solvents. The Journal of Physical Chemistry C, 2011. 115(12): p. 5140-5146.
30. Segets, D., et al., Analysis of Optical Absorbance Spectra for the Determination of ZnO Nanoparticle Size Distribution, Solubility, and Surface Energy. ACS Nano, 2009. 3(7): p. 1703-1710.
31. Bhushan, M., R. Jha, and R. Bhardwaj, Reduced band gap and diffusion controlled spherical n-type ZnS nanoparticles for absorption of UV-Vis region of solar spectrum. Journal of Physics and Chemistry of Solids, 2019. 135: p. 109021.
32. Gligorovski, S., et al., Environmental Implications of Hydroxyl Radicals (•OH). Chemical Reviews, 2015. 115(24): p. 13051-13092.
33. Feng, W. and D. Nansheng, Photochemistry of hydrolytic iron (III) species and photoinduced degradation of organic compounds. A minireview. Chemosphere, 2000. 41(8): p. 1137-1147.
34. Bhat, A.P. and P.R. Gogate, Degradation of nitrogen-containing hazardous compounds using advanced oxidation processes: A review on aliphatic and aromatic amines, dyes, and pesticides. Journal of Hazardous Materials, 2021. 403: p. 123657.
35. Guengerich, F.P. and F.K. Yoshimoto, Formation and Cleavage of C–C Bonds by Enzymatic Oxidation–Reduction Reactions. Chemical Reviews, 2018. 118(14): p. 6573-6655.
36. Fu, H., et al., Photochemistry of Dissolved Black Carbon Released from Biochar: Reactive Oxygen Species Generation and Phototransformation. Environmental Science & Technology, 2016. 50(3): p. 1218-1226.
37. Gong, J.-S., et al., Nitrilases in nitrile biocatalysis: recent progress and forthcoming research. Microbial Cell Factories, 2012. 11(1): p. 142.
38. Kitanosono, T., et al., Catalytic Organic Reactions in Water toward Sustainable Society. Chemical Reviews, 2018. 118(2): p. 679-746.
39. Lassoued, A., et al., Synthesis, photoluminescence and Magnetic properties of iron oxide (α-Fe2O3) nanoparticles through precipitation or hydrothermal methods. Physica E: Low-dimensional Systems and Nanostructures, 2018. 101: p. 212-219.
40. Roca, A.G., et al., Design strategies for shape-controlled magnetic iron oxide nanoparticles. Advanced Drug Delivery Reviews, 2019. 138: p. 68-104.
41. Liu, J., et al., Shape-controlled iron oxide nanocrystals: synthesis, magnetic properties and energy conversion applications. CrystEngComm, 2016. 18(34): p. 6303-6326.

42. Shaikh, K.R., et al., Exploring the effect of crystalline phase on photocatalytic, antimicrobial and antioxidant performance of magnetic iron oxide nanoparticles. Nano-Structures & Nano-Objects, 2024. 38: p. 101166.
43. Ali, A., et al., Synthesis, characterization, applications, and challenges of iron oxide nanoparticles. Nanotechnology, Science and Applications, 2016. 9(null): p. 49-67.
44. Pinet, S., et al., A SEM-based method to determine the mineralogical composition and the particle size distribution of suspended sediment. International Journal of Sediment Research, 2019. 34(2): p. 85-94.
45. Nemati, Z., et al., Improving the Heating Efficiency of Iron Oxide Nanoparticles by Tuning Their Shape and Size. The Journal of Physical Chemistry C, 2018. 122(4): p. 2367-2381.
46. Gupta, A.K. and M. Gupta, Synthesis and surface engineering of iron oxide nanoparticles for biomedical applications. Biomaterials, 2005. 26(18): p. 3995-4021.
47. Nagajyothi, P.C., et al., Green synthesis: Photocatalytic degradation of textile dyes using metal and metal oxide nanoparticles-latest trends and advancements. Critical Reviews in Environmental Science and Technology, 2020. 50(24): p. 2617-2723.
48. D'Souza, J.N., et al., An ensuing repercussion of solvent alteration on biological and photocatalytic efficacy of Emilia sonchifolia (L.) phytochemicals capped zinc oxide nanoparticles. Colloids and Surfaces A: Physicochemical and Engineering Aspects, 2021. 627: p. 127162.
49. Leskovac, A. and S. Petrović Pesticide Use and Degradation Strategies: Food Safety, Challenges and Perspectives. Foods, 2023. 12, DOI: 10.3390/foods12142709.
50. Trandafilović, L.V., et al., Enhanced photocatalytic degradation of methylene blue and methyl orange by ZnO:Eu nanoparticles. Applied Catalysis B: Environmental, 2017. 203: p. 740-752.
51. Vasantharaj, S., et al., Biosynthesis of iron oxide nanoparticles using leaf extract of Ruellia tuberosa: Antimicrobial properties and their applications in photocatalytic degradation. Journal of Photochemistry and Photobiology B: Biology, 2019. 192: p. 74-82.
52. Badmapriya, D. and I. Asharani, Dye degradation studies catalysed by green synthesized iron oxide nanoparticles. International Journal of ChemTech Research, 2016. 9(6): p. 409-416.
53. Bibi, I., et al., Green synthesis of iron oxide nanoparticles using pomegranate seeds extract and photocatalytic activity evaluation for the degradation of textile dye. Journal of Materials Research and Technology, 2019. 8(6): p. 6115-6124.
54. Adesibikan, A.A., et al., A review on sustainable photocatalytic degradation of agro-organochlorine and organophosphorus water pollutants using biogenic iron and iron oxide-based nanoarchitecture materials. Desalination and Water Treatment, 2024. 320: p. 100591.
55. Ebrahiminezhad, A., et al., Plant-Mediated Synthesis and Applications of Iron Nanoparticles. Molecular Biotechnology, 2018. 60(2): p. 154-168.
56. Martínez-Cabanas, M., et al., Green synthesis of iron oxide nanoparticles. Development of magnetic hybrid materials for efficient As(V) removal. Chemical Engineering Journal, 2016. 301: p. 83-91.

How to cite this article:
Niaz, A., Suleman, M., & Ullah, R. (2025). Green-Synthesized Iron Oxide Nanoparticles from Olive Leaves for Efficient Photocatalytic Degradation of Dyes and Chlorpyrifos. Journal of Chemistry and Environment, 4(2), 63–74.